Fermi-polaron problem: Diagrammatic Monte Carlo method for divergent sign-alternating series

Fermi-Polaron: Diagrammatic Monte Carlo for Divergent Sign-Alternating Series

Nikolay Prokof'ev[1,2] and Boris Svistunov[1,2]

[1]*Department of Physics, University of Massachusetts, Amherst, MA 01003, USA*
[2]*Russian Research Center "Kurchatov Institute", 123182 Moscow, Russia*

Diagrammatic Monte Carlo approach is applied to a problem of a single spin-down fermion resonantly interacting (we consider the universal limit of short-range interaction potential with divergent s-wave scattering length) with the sea of ideal spin-up fermions. On one hand, we develop a generic, sign-problem tolerant, method of exact numerical solution of polaron-type models. On the other hand, our solution is important for understanding the phase diagram and properties of the BCS-BEC crossover in the strongly imbalanced regime. This is the first, and possibly characteristic, example of how the Monte Carlo approach can be applied to a divergent sign-alternating diagrammatic series.

PACS numbers: 05.30.Fk, 05.10.Ln, 02.70.Ss

In this Letter we introduce a novel technique for studies of polaron type models which is equally important from both physical and technical points of view. On the physical side, we find a controllably-accurate numeric solution for the problem of a single spin-down fermion resonantly interacting with the sea of ideal spin-up fermions. This problem naturally arises in studies of the BCS-BEC crossover in the strongly imbalanced regime [1, 2]. In the case of stability of the dilute spin-down sub-system in the ideal spin-up fermi-sea, the solution of the single-particle problem would naturally define the phase diagram in the vicinity of the multicritical point (so-called M-point), discussed recently by Sachdev and Yang [3], where four different phases meat. Even if the M-point is thermodynamically unstable—as is actually suggested by the analysis of Giorgini and collaborators on the basis of their fixed-node Monte Carlo simulations [4]—the single-particle M-point, corresponding to the critical interaction strength at which the spin-down fermion forms a bound state with a spin-up fermion thus becoming a spin-zero composite boson, is of interest on its own. Also, for making a definitive theoretical conclusion about thermodynamic (in)stability of the dilute spin-down sub-system one still has to find an unbiased solution to the single-particle problem.

On the technical side, we solve the Fermi-polaron problem by diagrammatic Monte Carlo (MC) technique, which proved very efficient for electron-phonon polaron problems [5]. Though the diagrammatic series for the Fermi-polaron are quite similar, the crucial difference is that in the Fermi system we have to deal with the sign-alternating, divergent (at least for strong coupling) series. Under these conditions a direct summation of all relevant Feynman diagrams for the Green's functions is not possible, and one has to develop additional tools for (i) reducing the number of diagrams by calculating self-energies rather than Green's functions, and (ii) extrapolating MC results to the infinite diagram order for a divergent series. We find that the series for the Fermi-polaron are Riesz-summable and the numerically exact solution within the diagrammatic MC approach does exist. We believe that our findings are important in a much broader context since the diagrammatic MC approach to the many-body problem has essentially the same structure.

In what follows, we will be using the term 'polaron' in a narrow sense, i.e. only for the unbound fermionic spin-down excitation. For the composite boson we will be using the term 'molecule'. If polaron is a well-defined elementary excitation, its energy $E(\mathbf{p})$ can be extracted from the pole in the single-particle spin-down Green's function in the frequency-momentum representation, by solving the equation

$$[G_\downarrow^{(0)}(\omega = E(\mathbf{p}),\, \mathbf{p})]^{-1} \,=\, \Sigma_\downarrow(\omega = E(\mathbf{p}),\, \mathbf{p}) \;, \qquad (1)$$

where $G_\downarrow^{(0)}$ is the vacuum Green's function for the spin-down particle and $\Sigma_\downarrow$ is the self-energy of spin-down particle in the Fermi-sea of spin-up particles. In diagrammatic Monte Carlo we traditionally use the imaginary-time–momentum representation to circumvent the problem of dealing with the singular structure of free propagators and alleviate the sign problem. Remarkably, in order to find the polaron energy we do not have to perform a numeric analytic continuation from imaginary to real frequencies, because in the imaginary-time–momentum representation Eq. (1) translates into

$$[G_\downarrow^{(0)}(\omega = E(\mathbf{p}),\, \mathbf{p})]^{-1} \,=\, \int_0^\infty \Sigma_\downarrow(\tau,\, \mathbf{p}) \mathrm{e}^{E(\mathbf{p})\tau} d\tau \;. \qquad (2)$$

The equivalence of Eqs. (1) and (2) readily follows from the fact that for the spin-down particle there is a freedom of choosing the 'chemical potential' $\mu_\downarrow$ (for a single particle this is just a uniform external potential which does not affect its physical properties). This freedom can be utilized for fine-tuning $\mu_\downarrow = E(\mathbf{p})$, in which case the solution of Eq. (1) corresponds to zero frequency. Then, by noting that zero real frequency is the same as zero imaginary frequency, and utilizing the trivial dependence of self-energy on $\mu_\downarrow$, namely, $\Sigma_\downarrow(\tau,\, \mathbf{p},\, \mu_\downarrow) \,=\, \Sigma_\downarrow(\tau,\, \mathbf{p}) \mathrm{e}^{\mu_\downarrow \tau}$, one proves Eq. (2).

We obtain self-energy $\Sigma_\downarrow(\tau,\, \mathbf{p})$ by means of diagrammatic MC which works with standard diagrammatic expansions for Green's functions by interpreting them as a statistical ensemble. In our case, the diagrams are constructed from the following lines: (i) the already-mentioned vacuum propagator $G_\downarrow^{(0)}(\tau, p) = e^{(\mu_\downarrow - p^2/2m)\tau}$

FIG. 1: The first-order diagram for $\Sigma_\downarrow$, consisting of the T-matrix propagator (heavy dashed line) and spin-up propagator (solid arc).

FIG. 2: The first diagram for molecular self-energy K, consisting of one T-matrix propagator (heavy dashed line), two spin-up propagators (solid arcs), and two spin-down propagators (solid straight lines).

where m is the particle mass; it will be represented by thin horizontal straight lines, (ii) the spin-up propagators $G_\uparrow(\tau, p > k_F) = e^{(\epsilon_F - p^2/2m)\tau}$ and $G_\uparrow(\tau, p < k_F) = e^{-(\epsilon_F - p^2/2m)\tau}$ (where k_F and ϵ_F are the Fermi momentum and Fermi energy of spin-up particles); they are depicted with thin-line arcs, and (iii) the T-matrix propagator $\Gamma(\tau, p)$. The specifics of the resonant problem is that T-matrix has to be considered as a separate diagrammatic element which sums ladder diagrams for the short-range pair interaction potential. This summation takes the ultra-violet physics into account exactly and allows to express $\Gamma(\tau, p)$ in terms of the s-scattering length a. The ladder structure of diagrams absorbed in the T-matrix explains why we treat it as a 'pair propagator' and depict it with a (dashed heavy) line. The exact expression for $\Gamma(\tau, \mathbf{p})$ in the zero-range limit in the frequency-momentum representation reads

$$\Gamma^{-1}(\omega, p) \,=\, \frac{m}{4\pi a} \,-\, \frac{m}{8\pi}\sqrt{p^2 - 4m\eta} - \Pi(p, \eta)\;, \qquad (3)$$

$$\Pi(p, \eta) \,=\, \int_{q \le k_F} \frac{d\mathbf{q}/(2\pi)^3}{q^2/2m + (\mathbf{p}-\mathbf{q})^2/2m - \eta}\;. \qquad (4)$$

$$\eta \,=\, \omega + \varepsilon_F\;. \qquad (5)$$

As an illustration, in Fig. 1 we present the first-order diagram for $\Sigma_\downarrow$.

The energy of the molecule, $E_m(\mathbf{p})$, cannot be extracted from Eqs. (1), (2), because the corresponding pole exists only in the two-particle (spin-up + spin-down) or "pair" channel. Due to the fact that the resonant T-matrix is formally playing the role of a pair propagator, the theory of the molecular pole is analogous to the Dyson-equation theory of the polaron pole. Diagrammatically, it arises from the summation of geometric series of products $\Gamma K \Gamma K \Gamma K \ldots$ where K is the Γ-irreducible diagram in the two-particle channel—a direct analog of self-energy of the single-particle channel (see Fig. 2 for an illustration). Correspondingly, the molecular energy is found by solving an equation

$$\Gamma^{-1}(\omega = E_m(\mathbf{p}),\, \mathbf{p}) \,=\, \int_0^\infty K(\tau,\, \mathbf{p})\, \mathrm{e}^{E_m(\mathbf{p})\tau} d\tau\;. \qquad (6)$$

We found neither analytical expression for $\Gamma(\tau, p)$, nor fast way of tabulating it with high accuracy using inverse Laplace transform of the frequency-momentum representation Eq. (3). Instead, we applied recently-developed bold diagrammatic Monte Carlo (BMC) technique [6] to obtain $\Gamma(\tau, p)$ numerically, by relating it to the vacuum T-matrix the analytic expression for which in (τ, p)-representation is readily obtained. This was the first practical application of BMC, see Ref. [6] for details.

The updates we use for sampling the diagrammatic series do not differ dramatically from the ones described in literature, and we leave the corresponding discussion to a full-sized paper [7]. Instead, we concentrate on the convergence issues. In contrast to previous examples of diagrammatic Monte Carlo, the series for the resonant Fermi-polaron problem turns out to be divergent. However, the Cesàro-Riesz summation techniques fix the problem. For the quantity of interest—polaron or molecule self-energy—we construct the Cesàro-Riesz partial sums, $\Sigma(N_*) = \sum_{N=1}^{N_*} D_N F_N^{(N_*)}$, defined as sums of all diagrams up to order N_* [the diagram order, N, is defined by the number of spin-up propagators] with the N-th order terms being multiplied by the factor

$$F_N^{(N_*)} = [(N_* - N + 1)/N_*]^\delta\;, \qquad \text{(Cesàro-Riesz)}\;. \quad (7)$$

Here $\delta > 0$ is a fixed parameter ($\delta = 1$ corresponds to the Cesàro method). If the series is Riesz-summable, then the answer in the $N_* \to \infty$ limit does not depend on δ. The freedom of choosing the value of Riesz's exponent δ is used to optimize the convergence.

For the N_*-truncated and reweighed series we first determine the polaron and molecule energies and then study their dependence on N_* as $N_* \to \infty$. Figure 3 illustrates the procedure. The odd/even oscillations are very pronounced for $\delta = 1$ hinting at the absence of convergence of the original series but are strongly suppressed for larger values of δ. With $\delta = 4$ we were not able to resolve odd-even oscillations, but the smoothness of the curve here comes at the expense of increased curvature, which renders the extrapolation to the $1/N_* \to 0$ limit vulnerable to systematic errors. Empirically, we constructed a sort of generalized Cesàro-Riesz factor $F_N^{(N_*)}$ which leads to a much faster convergence (cf. Fig. 4); in what follows we refer to it as an *advanced* summation technique

$$F_N^{(N_*)} \,=\, C_{N_*} \sum_{m=N}^{N_*} \exp\left[-\frac{(N_*+1)^2}{m(N_*-m+1)}\right], \qquad (8)$$

$$C_{N_*}^{-1} \,=\, \sum_{m=1}^{N_*} \exp\left[-\frac{(N_*+1)^2}{m(N_*-m+1)}\right]. \qquad (9)$$

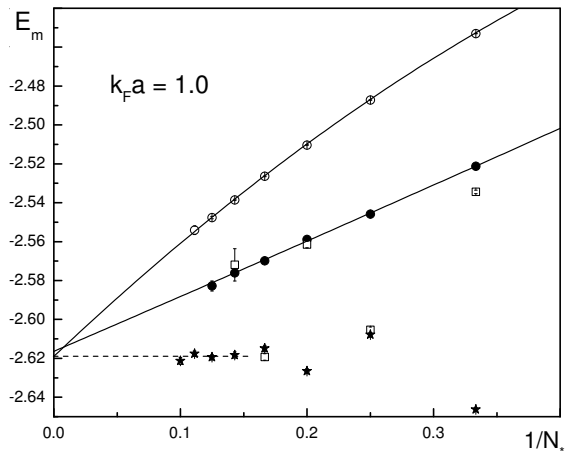

FIG. 3: The molecule energy (at $k_F\, a = 1$) as a function of truncation parameter N_* for different summation techniques: Cesàro (open squares), Riesz $\delta = 2$ (filled circles, fitted with the parabola $y = -2.6164 + 0.28013x + 0.01638x^2$), Riesz $\delta = 4$ (open circles, fitted with the parabola $y = -2.6190 + 0.61635x - 0.3515x^2$), advanced summation described in the text (stars). In the $\delta = 2$ case, the odd-even oscillations are strongly suppressed, as compared to Cesàro case, but still visible at higher resolution.

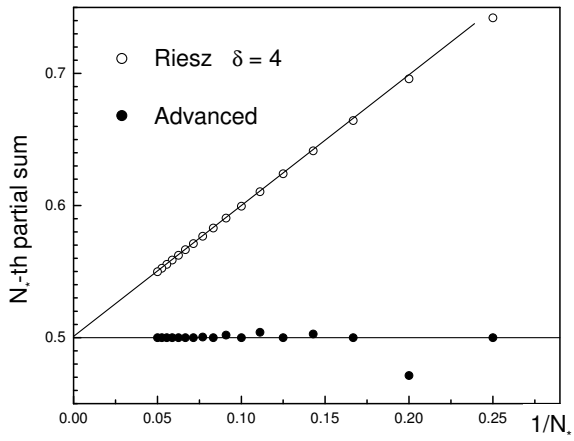

FIG. 4: Summing the Grandi series, $1-1+1-1+\ldots = 1/2$, by Riesz method and by the advanced method described in the text. The solid lines are to guide an eye.

For the molecular energy, the advanced summation demonstrates no visible linear slope in the $1/N_* \to 0$ limit. For the polaron energy, there is a small linear slope, but without visible curvature, see Fig. 5.

To ensure that both the code and data processing are error free, we check our answer for the molecule ground-state energy against the asymptotic solution

$$E_m = -\frac{1}{ma^2} - \varepsilon_F + \frac{2\pi\tilde{a}}{(2/3)m} n_\uparrow \qquad (k_F a \to 0)\,, \quad (10)$$

in which the first term in the r.h.s. is the binding energy

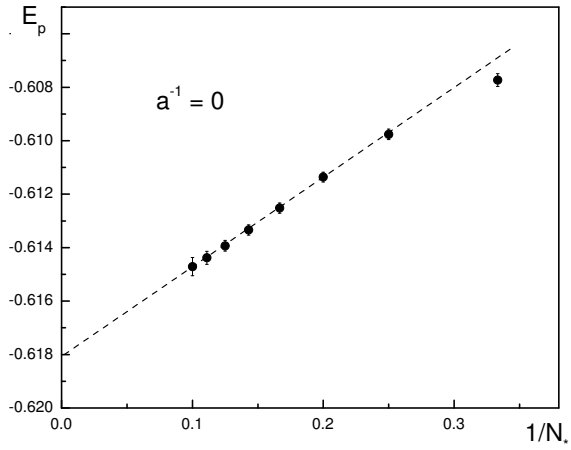

FIG. 5: The polaron energy (at the unitarity point $a^{-1} = 0$) as a function of truncation parameter N_* for the advance summation technique. The asymptotic behavior at $1/N_* \to 0$ is perfectly fit by a straight line.

of molecule in vacuum, the second term reflects finite chemical potential for spin-up fermions, and the third term comes from the mean-field interaction between the compact molecule and the remaining spin-up particles. Correspondingly, $\tilde{a} \approx 1.18a$ is the molecule-fermion s-scattering length [8]. The value of $\tilde{a}$ is based on the non-perturbative solution of the three-body problem, and thus provides a robust test to the entire numerical procedure of sampling divergent sign-alternating diagrammatic series. Our data are in a perfect agreement with the $\tilde{a} \approx 1.18a$ result within the statistical uncertainty of the order of 5%.

In Fig. 6, we show polaron and molecule energies in the region of $k_F a \sim 1$ where the nature of the quasiparticle state changes. The M-point is found to be at $(k_F a)_c = 1.11(2)$. The values of both polaron and molecule energies are in excellent agreement with the fixed-note Monte Carlo simulations [2, 4]. Interestingly, the polaron self-energy is nearly exhausted by the first-order diagram considered in Ref. [9], see also Fig. 5.

A comment is in order here on why the polaron (molecule) remains a good elementary excitation at $k_F a < (k_F a)_c$ ($k_F a > (k_F a)_c$) and the M-point is an exact crossing. In the limit of $k_F a \to (k_F a)_c$, this is guaranteed by the phase-space argument. The conservation of energy, momentum, and spin projection dictate that the leading decay channel involves four quasiparticles in the final state: the polaron decays into molecule, two holes and one spin-up particle; the molecule decays into a polaron, one hole, and two spin-up particles. Correspondingly, the decay width—proportional to the four-particle phase-space volume allowed by the conservation laws—gets negligibly small as compared to the energy difference $|E_m - E_p|$ at $k_F a \to (k_F a)_c$. Our numeric results show that $|E_p - E_m| \ll |E_p|, |E_m|$ even when $k_F a$ is substantially different from $(k_F a)_c$. Since the phase-space

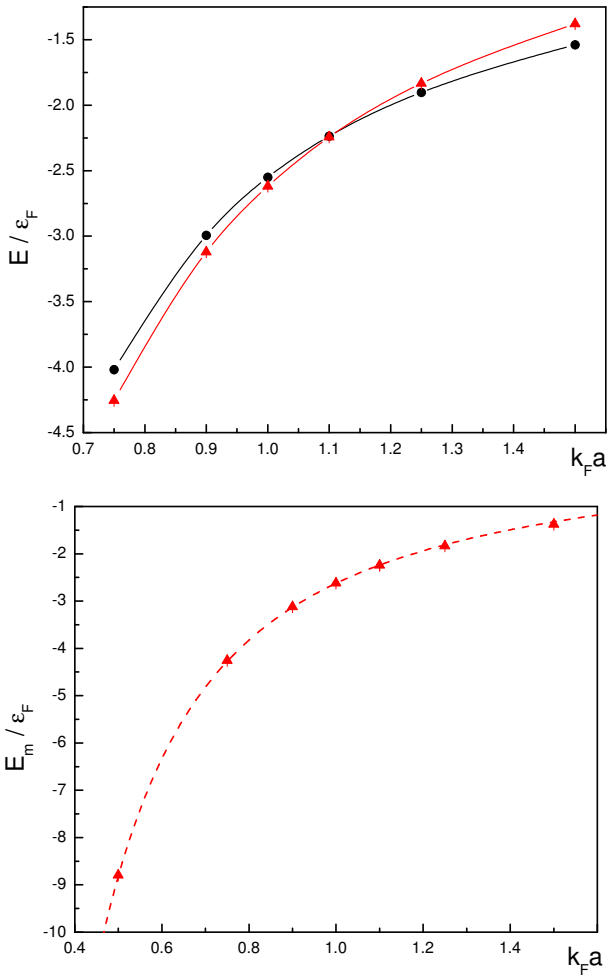

FIG. 6: Polaron (circles) and molecule (triangles) energies (in units of ε_F) as functions of $k_F a$. The dashed line on the lower panel corresponds to Eq. (10).

volume is determined by $|E_p - E_m|$, this explains why the width of the decaying quasiparticle remains small and goes beyond our numeric resolution.

The data for the effective mass is presented in Fig. (7). As expected, at the crossing point the effective mass curve is discontinuous. Note that good agreement with Eq. (10) for E_m at all couplings up to the M-point is slightly misleading since Eq. (10) assumes that molecules are compact and their mass is $2m$. The actual effective mass is significantly enhanced in the vicinity of the M-point.

Summarizing, the problem of resonant Fermi-polaron has been solved by diagrammatic MC. In particular, the point where the groundstate switches from the single-particle (fermionic) sector to two-particle (bosonic) sector is found to be at $k_F a = 1.11(2)$. On the computational side, it has been discovered that while the diagrammatic series is divergent, the fermionic sign-alternation of the diagrams renders the series summable by the Cesàro-Riesz-type methods and suitable for the diagrammatic

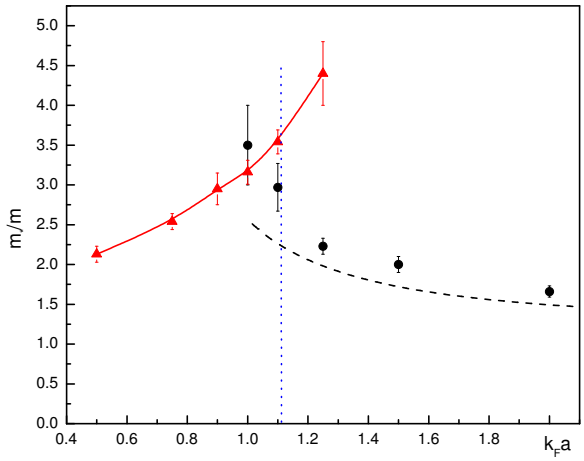

FIG. 7: Polaron (circles) and molecule (triangles) effective mass (in units of m) as functions of $k_F a$. The vertical dotted line stands for $(k_F a)_c = 1.11$. The dashed line is the contribution from the first diagram [9].

MC routine. Whether this *sign blessing* is a specific feature of the problem solved here, or a generic feature of fermionic and, possibly, other diagrammatic expansions, is a major question which we will address in future.

We are grateful to C. Lobo, S. Giorgini, and R. Combescot for valuable discussions and data exchange. The work was supported by the National Science Foundation under Grants PHY-0426881 and PHY-0653183. We also acknowledge a support from KITP, Santa Barbara (under NSF Grant PHY05-51164) and PITP, Vancouver.

[1] A. Bulgac and M. Forbes, Phys. Rev. A **75**, 031605 (2007).
[2] C. Lobo, A. Recati, S. Giorgini, and S. Stringari, Phys. Rev. Lett. **97**, 200403 (2006).
[3] S. Sachdev and K. Yang, Phys. Rev. B **73**, 174504 (2006).
[4] Stefano Giorgini, privite communication.
[5] N.V. Prokof'ev and B.V. Svistunov, Phys. Rev. Lett. **81**, 2514 (1998); A.S. Mishchenko, N.V. Prokof'ev, A. Sakamoto, and B.V. Svistunov, Phys. Rev. B **62**, 6317 (2000).
[6] N. Prokof'ev and B. Svistunov, arXiv:cond-mat/0702555.
[7] N. Prokof'ev and B. Svistunov, in preparation.
[8] G.V. Skorniakov and K.A. Ter-Martirosian, Zh. Eksp. Teor. Fiz. **31**, 775 (1956) [Sov. Phys. JETP **4**, 648 (1957)].
[9] R. Combescot, A. Recati, C. Lobo, and F. Chevy, Phys. Rev. Lett. **98**, 180402 (2007).